Structural Model of Silica Nanowire Assembled from a Highly Stable $(SiO_2)_8$ Unit

Dongju Zhang[†] and R. Q. Zhang*

Center of Super-Diamond and Advanced Films (COSDAF) and Department of Physics and Materials Science, City University of Hong Kong, Hong Kong SAR, China

Received: May 20, 2005; In Final Form: November 27, 2005

The ground-state structures of silica clusters $(SiO_2)_n$ for $n = 1-8$ were studied by performing calculations at the B3LYP/6-311+G(d) level of density functional theory. The results indicate that the growth mode of a silica nanowire based on small silica clusters may change at different wire lengths. A linear chain might be assembled from the smallest clusters of rhombic two-membered ring (2MR) with $n \leq 5$, while the growth motif changes at $n = 6$ into a more compact form composed of three-membered-rings (3MRs). The 3MR-containing structures become energetically favorable configurations for even longer silica clusters. In particular, the closed molecular ring consisting of 3MRs at $n = 8$ (i.e., $(SiO_2)_8$) with a high symmetry shows extreme energetic stability and relatively high chemical reactivity and thus is considered to be an important building block to assemble into silica nanowires. The relative stability of so-assembled silica nanowires were evaluated and compared with the models of silica nanowires in the literature.

1. Introduction

Silica is an important material in many technological and scientific areas.[1] In the past decades, considerable progress has been made in growing one-dimensional (1D) nanomaterials of silica, including nanowires[2−7] and nanotubes,[8−17] because of their potential applications in electronics, optics, and nanodevices. However, only a few experimental and theoretical studies have been reported on the atomic and electronic structures of these materials and on their nucleation and growth mechanisms, despite the success in their synthesis with a variety of methods, including laser ablation[2] for nanowires and the porous or solid rodlike template approach[8,9] for nanotubes. As the basic building blocks of these 1D nanomaterials, silica nanoparticles and clusters have also attracted a great deal of experimental[18−27] and theoretical[28−49] interests. Extensive efforts have been devoted to determining the structures for $(SiO_2)_n$ with $n < 10$[32−37] in recent years. For example, Harkless et al.[31] have performed extensive searches to locate possible stable structures of $(SiO_2)_n$ ($n = 1-8$) using molecular dynamics simulations and an empirical pairwise interaction potential. Nayak et al.[32] have carried out calculations for $(SiO_2)_n$ ($n = 1-6$) at the generalized gradient approximation (GGA) level of density functional theory (DFT) using Becke form of the exchange functional and Perdew-Wang expression of the correlation functional. Recently, Flikkema and Bromley[38,39] reported the lowest energy structures of $(SiO_2)_n$ with $n = 6-12$ at the B3LYP/ 6-31G(d) level of theory, based on the results obtained using the Basin Hopping global optimization algorithm[40] and their newly fitted interatomic potential for nanoscale silica. The predicted ground-state structures for $n = 7-8$ are different from those by Harkless et al.[31] A systematic theoretical study of the ground state structures for small silica clusters at a higher level of theory is still needed, as the revealed or confirmed structural motifs not only enrich the database of silica clusters but also provide important structural basis of the nanosized clusters to assemble into 1D nanomaterials. With study of these most basic gas-phase silica species via quantum chemical calculations, insight into the characteristics of the geometries and their transitions from one motif to another, and therefore the growth mechanism of silica nanoscale materials, would be provided.

Recently, we proposed a structural model of 1D thin silica nanowires[50] based on spiro union two-membered-ring (2MR) units. As revealed by DFT calculations, our silica nanowire is energetically favorable, thermally stable, and chemically reactive at the tip. Given the frequent occurrence of three-membered rings (3MRs) in small- and medium-sized silica clusters,[39,43,45,49] they can be expected to be assembled into silica nanowires. The formed 3MR-based nanowires would be slightly thicker than those assembled from the spiro union 2MR units.[50] Interestingly, a silica cluster, $(SiO_2)_8$, has been shown to be magic by Flikkema et al.[39] The geometrical structure of the ground state $(SiO_2)_8$ presents a high symmetry with reactive ends of Si═O groups, making it easy to be assembled into larger linearly extended clusters and showing the possibility to act as the building block of 1D silica nanowires.

In the present work, we aim at (I) searching for and evaluating the geometrical structures of the ground state $(SiO_2)_n$ ($n \leq 8$), (II) revealing the motif transition of silica clusters in the growth, (III) presenting a growth model of 1D silica nanowires, and (IV) further comparing their relative stabilities with the models reported earlier.

2. Cluster Models and Computational Details

The silica structures studied in this work include (1) the smallest ($1 \leq n \leq 8$), (2) medium- ($8 < n \leq 24$), and (3) larger sized ($24 < n \leq 72$) clusters. The geometric structures of the first set are taken from the literature (for $n = 1-5$) or designed (for $n = 6-8$) by considering (i) basic 4- and 2-fold bonding principles for Si and O atoms, respectively, (ii) two-, three-, and four-membered ring distributions, and (iii) the number of Si−O bond defects. The second and third sets of silica clusters were assembled from the most stable isomer of $(SiO_2)_8$, and

* To whom correspondence should be addressed. E-mail: aprqz@cityu.edu.hk.

† On leave from School of Chemistry and Chemical Engineering, Shandong University, Jinan, 250100, P.R. China.

10.1021/jp052643c CCC: $33.50
Published on Web 12/31/2005

thus they possess similar atomic structures but with different numbers of the basic units.

For the smallest clusters, $(SiO_2)_n$ ($n = 1-8$), we first performed simulated annealing simulations to search for their possible minima at room temperature near the starting configuration. Such an approach has been widely used in practice for searching for the global minimum of a system on its potential energy surface. The molecular dynamics simulation was run for 5 ps for each cluster at 5000 K with a time step of 1 fs using an efficient ab initio code known as SIESTA 1.3 code.[51] Afterward, the system was cooled to 300 K with a temperature decrement of 10 K in each step. To maximize the possibility of obtaining the global minimum, we performed at least three different simulated annealing processes for each cluster. The preponderant configurations obtained with a simulated annealing procedure were further optimized using the GAUSSIAN 98 program package[52] at the B3LYP/6-311+G(d) level of theory. The approach adopts the popular hybrid exchange-correlation functionals,[53,54] with a 6-311+G(d) basis set, a split-valence atomic basis set supplemented by a polarization function and a diffuse function. The accuracy of the level of theory chosen imparted by the electron correlation and the large basis set is expected to be sufficient to determine the relative stabilities of silica clusters. Bromley et al.[46] have shown that this level of theory well reproduces experimentally determined properties of silica nanoclusters. To obtain unbiased local-minimum structures of these small silica clusters, full geometry optimization calculations without any symmetry constraints were first conducted at the chosen level of theory. Then, the initial structures were optimized again by keeping the point-group symmetry of the clusters. The optimized structures were further subjected to the calculations for harmonic vibrational frequencies at the same level of theory, ensuring that they are real minima on the potential energy surfaces (PESs).

For the medium-sized clusters ($8 \le n \le 24$), our calculations were carried out using the same theory but with a smaller basis set 6-31G(d) in order to reduce the computational cost, whereas for the larger-sized ($24 < n \le 72$) clusters we performed DFT calculations using the Perdew-Burke-Ernzerhof's GGA[55] with the double-ζ plus polarization orbital (DZP) implemented in SIESTA 1.3 code.[51] The reliability of this method for determining geometries and relative energetics of silica clusters have been established in our recent work.[45] Our calculations showed that the SIESTA calculations can give reasonably accurate geometries and relative energetics of silica clusters compared to the results of high-level DFT calculations.

3. Results and Discussion

The energetic stability of the silica clusters was evaluated using the binding energy (E_b) per SiO_2 unit, which is defined as the energy difference between the total energy of a cluster and the corresponding isolated monomers, as given by eq 1,

$$E_b = \{E[(SiO_2)_n] - nE(SiO_2)\}/n \quad (1)$$

where $E(SiO_2)$ and $E[(SiO_2)_n]$ are the energies of monomer SiO_2 and its cluster $(SiO_2)_n$. This energy index is equivalent to the strain energy relative to α-silica used in our previous work[45] in evaluating the relative stability of silica clusters.

3.1. $(SiO)_n$ Clusters for $n = 1-5$. For $(SiO_2)_n$ ($n = 1-5$), a number of low-energy isomers proposed in the literature were re-examined, including those proposed by Harkless et al.[31] and Nayak et al.[32] As has been revealed earlier, the ground state of SiO_2 monomer has a linear structure with $D_{\infty h}$ symmetry, while those of four other small oligomers (dimer, trimer, tetramer, and pentamer) are all 2MR chain, indicating a trend to assemble into a 1D structure. However, this simple growth principle will not be applicable for $n > 5$, as will be seen in the next section. The dimer and tetramer have D_{2h} symmetries, and the trimer and pentamer have D_{2d} symmetries. The binding energies of these oligomers against SiO_2 monomer are 1.817, 2.602, 2.985, and 2.911 eV, respectively, showing a trend of monotonic increase. These values are close to those predicted by Nayak et al.,[32] but smaller than those by Harkless et al.[31] The large stability of these 2MR chains is related to their small fractions of nonbridging oxygen (NBO) atoms. In fact, such 2MR structures have been confirmed to exist not only in silica-*w* at high temperature[56] but also in Si−O−plasma reactions and can also be formed via the condensation of vicinal hydroxyls or the thermodynamic rearrangement of the pure silica structure at the surfaces of amorphous and crystalline silica and at high temperature.[57−62]

Some energetically competitive isomers for $(SiO_2)_n$ ($n = 3-5$) were also calculated in the present work. The 3MR isomer of the trimer was found to have a planar D_{3h} structure and to be energetically less favorable than the 2MR chain (−2.438 vs −2.602 eV), due to its larger number of NBO atoms (3 vs 2). Similarly, the next higher energy isomers for the tetramer and pentamer have been identified to be Harkless's C_{2v} structure[31] (a 2MR combined with a 3MR) and Nayak's D_{2d} structure[32] (consisting of two mutually perpendicular 3MRs), respectively. They are less stable by 0.074 and 0.108 eV in E_b than the corresponding ground states, respectively.

3.2. $(SiO_2)_n$ Clusters for $n = 6-8$. The number of possible geometries of a cluster is expected to grow exponentially with increasing cluster size. It is a difficult task to search for the global minima on the respective PESs for large clusters by first-principles calculations. However, for the present $(SiO_2)_n$ ($n = 6-8$) clusters, some possible stable and metastable structures can be predicted by considering the basic building principles for silica clusters described above. Their initial structures include the 2MR molecular rings and various hybridized fragments by two-, three-, and four-MRs. Compared with the extreme 2MRs, the appearances of 3MR, 4MR, and even 5MR in these slightly larger clusters seem to reduce intrinsic ring strain. However, their larger numbers of NBO atoms play an adverse role in stabilizing their structures. Thus, searching for an appropriate compromise or crossover of these two contrary factors would be important to establish the low-energy isomers of silica clusters. In the present work, we designed 18, 25, and 36 starting geometries for $n = 6$, 7, and 8, respectively. After the simulated annealing, we obtained 52 and 78 and 103 local minima from these three sets. Figure 1 shows several energetically most stable structures optimized at the B3LYP/6-31G(d) level of theory.

For $(SiO_2)_6$, our calculations have identified two more stable structures, **6a** and **6b**. The isomer **6a**, which has not been reported before, turned out to be the lowest energy structure. This structure consists of one 3MR and three 2MRs by sharing Si vertexes, a most compact structure with a quite different geometry from the 2MR chain, **6b**. It has D_{3h} symmetry and is energetically slightly more stable compared with the linear 2MR chains (D_{2h}), the ground state of $(SiO_2)_6$ revealed in the GGA calculations by Nayak et al.[32] In contrast, the structure **6d** (D_{2h}), which corresponds to that of Harkless et al.[31] and can be viewed as two 4MRs combined by sharing a pair of Si atoms, was found to be less stable by 0.075 eV in E_b than **6a**. The result indicates that the intrinsic internal strain in 2MRs becomes a crucial factor for the destabilization of silica clusters with $n \ge 6$, making the

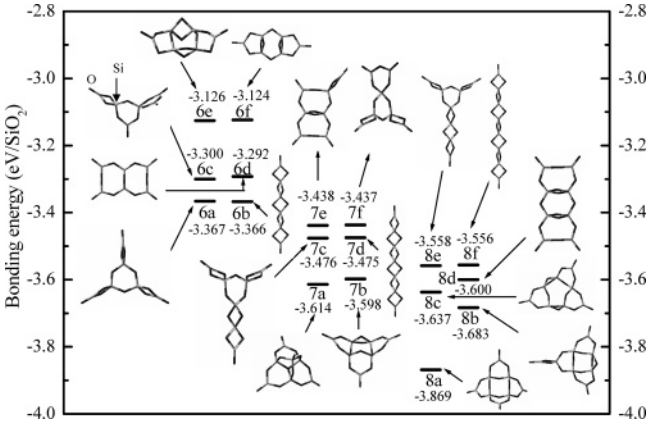

Figure 1. Geometries and binding energies of the ground state and the higher energy isomers for $(SiO_2)_n$ ($n = 6-8$) clusters calculated at the B3LYP/6-311+G(d) level. Light gray sticks depart from Si atoms and dark gray sticks from O atoms.

growth motif of silica clusters changed at $n = 6$, from the extended 2MR chains to a more compact structure. Three other structures, **6c** (C_s), **6e** (C_{2v}), and **6f** (D_{2h}), have also been identified as the low-energy isomers of $(SiO_2)_6$, and their E_b's are higher by 0.067, 0.241, and 0.243 eV than that of the ground-state structure, respectively. Although the structures **6e** and **6f** possess smaller numbers of NBO atoms, the tetrahedral bonds of the Si atoms in these structures are seriously distorted, leading to the decrease of their stabilities.

For $(SiO_2)_7$, a C_{3v} isomer, as shown in Figure 1 (**7a**), which was found to be the second stable structure recently by Flikkema and Bromley,[38,39] has been identified as the ground-state structure in this work. It consists of pure 3MRs and contains an overcoordinated NBO atom. The second lowest energy isomer is the **7b** structure with C_s symmetry, which involves three 3MRs and one 2MR with three NBO atoms. The third and fourth less stable isomers, **7c** and **7d** with C_{2v} and D_{2d} symmetries, have comparable stabilities. The last two isomers, **7e** and **7f**, are the least stable among the six and have C_1 and C_{2v} symmetries. It should be noted that Harkless et al. have identified **7e** as the ground state of $(SiO_2)_7$. However, this isomer was found to be energetically less favorable by 0.176 eV in E_b than **7a** in the present calculations. From the relative stabilities of these six low-energy isomers, it is clear that the most compact C_{3v} isomer (**7a**), rather than the extended 2MR chain (**7d**), is the most stable structure. This compact feature in structure continues to be advantageous when increasing the cluster size. For $(SiO_2)_8$, our calculations suggest that the isomer **8a**, with a closed molecular ring consisting of four 3MRs with D_{2d} symmetry, is the global minimum on the PES. This agrees with Flikkema's recent finding.[39] Harkless et al.[31] have identified an octamer, **8d** (D_{2d} symmetry), as the most stable structure. However, in the present calculations, it is less stable by 0.269 eV in E_b than **8a**. The next higher energy isomer, **8b** (C_s symmetry), is a simple extension of **7b**, consisting of a SiO_2 monomer that attaches to the end oxygen atom of a 3MR of **7b** with two oxygen atoms joining in a 2MR. The isomer **8c** can be viewed topologically as another isomer growing from **7b** upon replacement of its shared 3MR Si vertex with a pair of Si atoms that are themselves connected across the cluster by a double oxygen bridge. The isomers **8b** and **8c** are less stable by 0.186 and 0.232 eV in E_b than **8a**, respectively, due to the appearances of two 2MRs. Our calculations indicate that the stability of the isomers for $(SiO_2)_8$ decreases with increasing the number of 2MRs. Isomers **8e** (C_{2v} symmetry) and **8f** (D_{2h} symmetry) that possess five and seven 2MRs respectively were found to be energetically very unfavorable, although they have relatively fewer number of NBO atoms.

From the results described above, it is clear that the geometries of the ground-state isomers for $(SiO_2)_n$ ($n = 1-8$) are diverse. The simple growth principle for $n \leq 5$, i.e., the extension of 2MR chains, is no longer the optimal form for larger clusters. However, a clue of the motif change for these smallest silica clusters has been clearly drawn out from our calculations: extended 2MR chain motifs for $n \leq 5$ change into more compact 3MR-involved motifs at $n = 6$ and into pure 3MR-based motifs at $n = 7$ and 8. This fact indicates that 3MR could be the favorable building block for larger silica clusters.

3.3. Structural Model of Silica Nanowires Based on the Highly Stable $(SiO_2)_8$. The geometrical features of the ground states for the smallest silica clusters $(SiO_2)_n$ ($n = 1-8$) are important for understanding the structures and bonding properties of larger silica clusters. These structures are expected to be more abundant species and can act as nucleation centers or precursors for forming larger clusters. In particular, the ground-state structure of $(SiO_2)_8$, **8a**, has highly symmetric geometry and much higher stability than other isomers, making it a possible candidate to be assembled into 1D nanostructures. The high stability of this structure of $(SiO_2)_8$ has also been noted in the very recent work by Flikkema and Bromley,[39] where they proposed $(SiO_2)_8$ as a "magic" cluster of silica. Its unusually high stability is related to its unique geometrical feature: a closed molecular ring containing four relatively relaxed SiO_4 quasi-tetrahedral units, where four 3MRs symmetrically extend above and below the plane that consists of four Si atoms. For each SiO_4 unit, the O−Si−O angles are 104.0°, 104.0°, 107.8°, and 119.6°, respectively, closer to the angles in crystalline α-quartz (108.81°, 108.93°, 109.24°, and 110.52°)[63] than the corresponding SiO_4 unit consisting of 2MRs (about 90°). Further, the Si−O−Si angles in this 3MR-based molecular ring were determined to be 119.2° and 130.3°, which are also much larger than those in the 2MR chains (close to 90°), although smaller compared with that in α-quartz (143.73°). These relatively unrestrained angles in **8a** make it energetically more favorable and hence a higher population in the clusters than other isomers. To provide additional unique information on this stable motif, Figure 2 compares its IR spectrum, scaled with a factor of 0.9679,[64] with the spectra of the other five isomers of $(SiO_2)_8$. We found that this 3MR-based motif, **8a**, has a prominent, sharp peak at 1072 cm^{-1} [panel (a) of Figure 2], which is assigned to asymmetrical stretching motions of the Si−O−Si bonds. This characteristic is clearly distinguishable from the characteristic peak of the 2MR molecular chain (**8f**) at 892 cm^{-1} [panel (f) of Figure 2], and also from those of the other four isomers of $(SiO_2)_8$, **8b**, **8c**, **8d**, and **8e**, which only present broad and weak IR spectra in the vicinity of this characteristic peak, as shown in the panels (b), (c), (d), and (e) of Figure 2, respectively. The sharp peak of $(SiO_2)_8$ at 1072 cm^{-1} matches well with the experimental IR spectrum on fumed silica (a synthetic amorphous silicon dioxide produced by burning silicon tetrachloride in an oxygen−hydrogen flame) heated at 900−1000 °C, where a rather narrow band at ∼1000 cm^{-1} was observed as compared with bulk silica.[27] This fact suggests that the 3MR-based molecular ring (**8a**) may be the main component in fumed silica. It is noted that this 3MR-ring motif also displays weaker modes at ∼1300 cm^{-1}, similar to the cases of five other isomers. These modes are attributed to the vibrations of defective Si−O groups at the ends of the clusters.

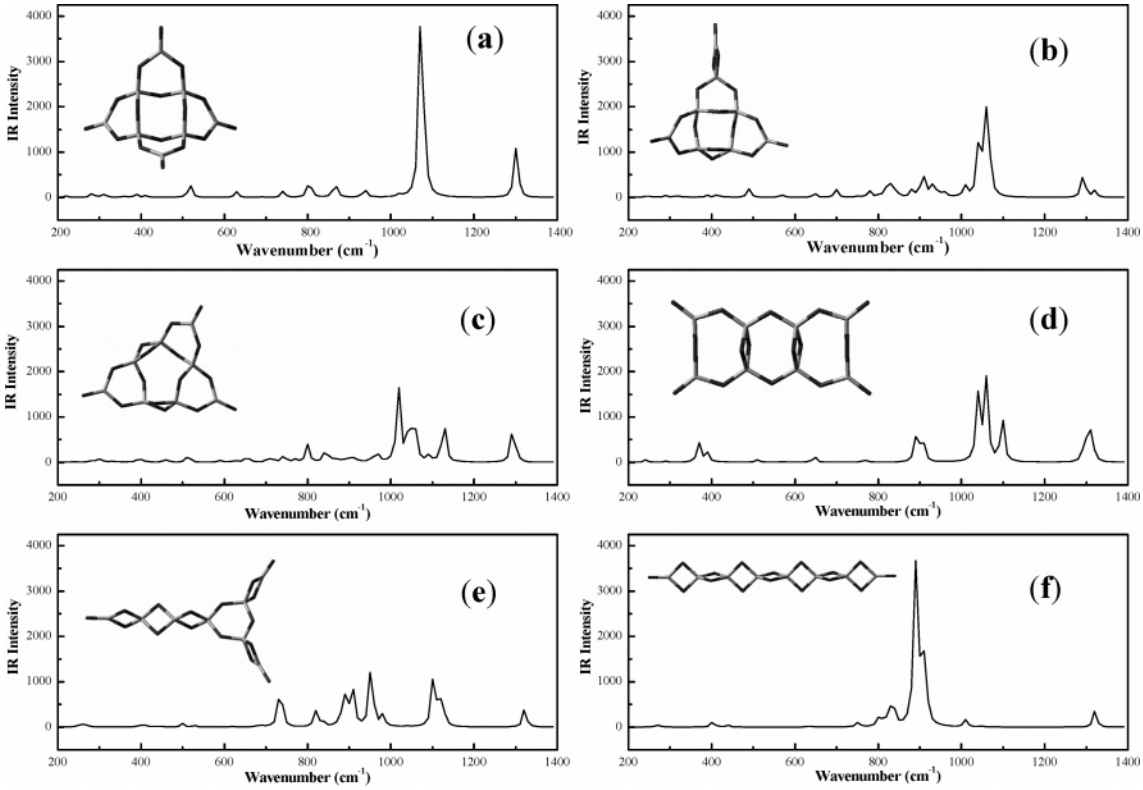

Figure 2. Scaled IR spectra for six isomers of $(SiO_2)_8$ from the B3LYP/6-311+G(d) calculations.

We have also tested the thermal stability of this 3MR-ring motif by performing DFT molecular dynamics simulations using SIESTA code at several temperatures, including 500, 1000, 1500, 2000, and 3000 K, with a time step of 1 fs for a total of 1000 steps. Atomic forces are calculated using the Hellmann-Feymann theorem; Newton's equations are integrated by means of the Verlet algorithm. We found that the optimized geometry retains its initial connectivity throughout the whole simulation even at 3000 K, which is far higher than the synthesis conditions (~1000 K). It indicates that the 3MR molecular ring is thermally stable and very resistant to collapse or rupture.

Further, we investigated the electronic property of the stable 3MR-ring motif. The energy gap between the highest occupied molecular orbital (HOMO) and the lowest unoccupied molecular orbital (LUMO) is 5.842 eV, smaller than that of the corresponding 2MR molecular chain (**8f**), 6.318 eV. It is well-known that the energy gap is a signature of the chemical reactivity of a system: a small gap would indicate a high reactivity. Thus, the 3MR-ring motif is expected to have higher chemical reactivity. This can be attributed to its larger number of Si═O groups, which act as defect sites of the structures and hence the reactive centers, as shown by the isodensity surfaces of its HOMO and LUMO states in Figure 3. Clearly, both the HOMO and LUMO highly localize on the O and Si atoms at the Si═O groups, making these regions highly active. This fact indicates that the 3MR-ring motifs easily bind into larger clusters via their mutual coalescence of the end Si═O groups.

A new structural type of silica clusters appears once the3MR-ring motifs are assembled into larger size. Figure 4 shows three representative structures of the clusters assembled from this basic unit. These structures contain two, three, and nine units of the $(SiO_2)_8$ ring, respectively. They possess unique geometrical features: two basic units of $(SiO_2)_8$ link into a prolate, rhombus-like wire; the adjacent two units are mutually perpendicular to each other. The structure extends in a straight way. Note that the two 2MRs naturally appear between two basic motifs. To

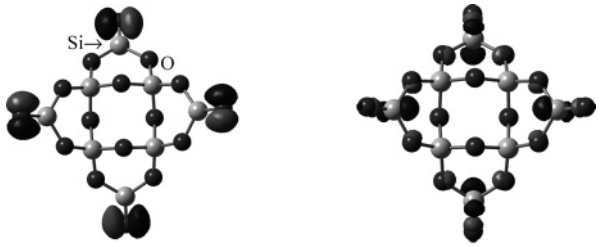

Figure 3. Isodensity surfaces of the HOMO and LUMO states for the most stable 3MR-ring motif of $(SiO_2)_8$. The dark gray balls represent oxygen atoms, and light gray balls represent silicon atoms.

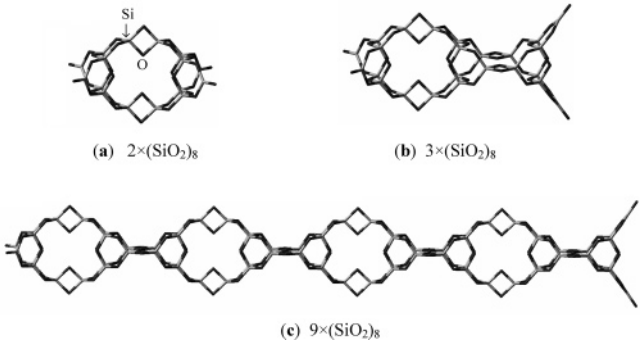

Figure 4. Stable geometries of the silica clusters assembled form the most stable 3MR-ring motif of $(SiO_2)_8$. The panels (a) and (b) contain two and three $(SiO_2)_8$ units, respectively, and were optimized using GAUSSIAN 98 code at the B3LYP/6-31G(d) level and the panel (c) was optimized using only SIESTA code at the GGA/DPZ level due to its larger size (nine $(SiO_2)_8$ units). Light gray sticks depart from Si atoms and dark gray sticks from O atoms.

test the structural and energetic stabilities of these elongated clusters, we optimized their structures using GAUSSIAN 98 code at the B3LYP/6-31G(d) level of theory for the clusters

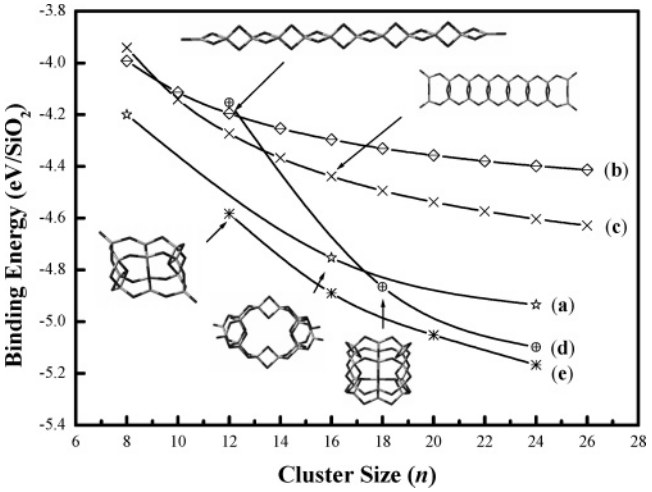

Figure 5. Monomer binding energy (E_b) of the silica clusters calculated at the B3LYP/6-31G(d) level as a function of the cluster size, *n*, for (a) the new structures proposed in this work, (b) the 2MR molecular chains,[46] (c) the spiro union 2MR molecular chains,[50] (d) the double six-ring wires, and (e) the double four-ring wires. Several representative structures (one from each type) of the silica clusters are included as insets in the figure.

with $n = 16$ and $n = 24$, and using SIESTA code at the GGA/DZP level of theory for those with $24 < n \leq 72$. The optimized geometries and computed E_b at the B3LYP/6-31G(d) level of theory were shown in Figures 4 and 5, respectively. The geometries of these clusters are not apparently different from the initially assembled structures, indicating their intrinsic structural stabilities. To confirm this point, we distorted the initial structures to bended forms. Upon the geometric optimization, the final geometries converged to those shown in Figure 4. Our SIESTA calculations reveal that the straight chain trend to grow continuously, as shown with the largest clusters of *n* up to 72 studied in this work (Figure 4c). From these results, a structural model of the silica nanowires emerges clearly. In Figure 5, the E_b's of the new silica structures (curve (a) in Figure 5) were compared with those of silica nanowires of similar diameters in the literature, including the thinnest 2MR molecular chain[46] (curve (b) in Figure 5), the spiro union 2MR molecular chain[50] (curve (c) in Figure 5), the double six-ring nanowire[65] (curve (d)), and the double four-ring nanowire built from the ground-state building unit of $(SiO_2)_{12}$[39] (curve (e)). Clearly, the present silica clusters are much more stable in E_b than the 2MR chain and spiro union 2MR chain. For example, the silica rods for $n = 16$ and $n = 24$ are respectively more stable by 0.314 and 0.349 eV than the corresponding spiro union 2MR molecular chains, by 0.424 and 0.456 eV than the corresponding edge-shared 2MR molecular rings, and by 0.456 and 0.537 eV than the corresponding edge-shared 2MR molecular chains. Compared with the double six-ring model and the double four-ring model, however, the present 3MR-based silica nanowire model is energetically less favorable, as shown in Figure 5 according to our calculated binding energies. This can be attributed to the relatively larger strains in 3MRs than in 4MRs and 6MRs. Experimentally, silica nanowires were synthesized via many methods, such as excimer laser ablation, carbothermal reduction, and catalyzed thermal decomposition. Therefore, the silica nanowires synthesized at given conditions are expected to possess characteristic microstructures. In other words, the structures of synthetic silica nanowires depend on the given condition. It should be noted that ground-state structures are not necessarily formed, but metastable structures in real 1D nanomaterials,[48] as confirmed by recent experiments.[66] Based on these facts, we consider the present 3MR-based silica model as one of the reasonable structural models of 1D silica nanowires, even though it is not energetically the most favorable structure. We believe that the present results will provide valuable additional information for understanding the nucleation and growth mechanisms of the silica nanowires.

To reveal the electronic properties and the chemical stability, we examined the HOMO−LUMO gap of these silica clusters varying with the cluster size using SIESTA code. The calculated results indicate that the gap increases with increasing length of the clusters and levels off to a constant, 4.50 eV at $n = 48$. This value is smaller than that of α-quartz, 6.03 eV calculated at the same level of theory, indicating that the proposed silica nanowires may possess electronic and optical properties different from α-quartz and hence can be expected to find novel applications in nanodevices.

4. Summary and Conclusions

We have evaluated the ground-state structures of the silica clusters for $n = 1-8$ by performing DFT calculations at the B3LYP/6-311+G(d) level of theory. The ground states of the monomer and dimer present linear and rhombic 2MR structures, respectively, while those for trimer, tetramer, and pentamer are simply continuous extensions of the rhombic 2MR ring. However, this simple growth mode is no longer applicable at $n = 6$, and after that the 3MR-containing structures become energetically preponderant configurations. The magic cluster $(SiO_2)_8$ is particularly appropriate to act as the building block of 1D silica nanowires.

Acknowledgment. The work described in this paper is jointly supported by grants from the Research Grants Council of the Hong Kong Special Administrative Region, China [project No. CityU 1011/01P and project No. CityU 1033/00P], CAS-Croucher Funding Scheme for Joint Laboratories and Chinese Academy of Sciences, China. We are grateful to the referee for the constructive suggestions which were used to improve this work.

References and Notes

(1) See, for example: *Physics and Chemistry of Finite System: From Clusters to Crystals*; Jena P., Khanna, S. N., Rao, B. K., Eds.; Kluwer Academic Pulishers: Boston, 1992; Vols. I and II.

(2) Yu, D. P.; Hang, Q. L.; Ding, Y.; Zhang, H. Z.; Bai, Z. G.; Wang, J. J.; Zou, Y. H.; Qian, W.; Xiong, G. C.; Feng, S. Q. *Appl. Phys. Lett.* **1998**, *73*, 3076.

(3) Takikawa, H.; Yatsuki, M.; Sakakibara, T. *Jpn. J. Appl. Phys.* **1999**, *38*, L401.

(4) Wu, X. C.; Song, W. H.; Wang, K. Y.; Hu, T.; Zhao, B.; Sun, Y. P.; Du, J. J. *Chem. Phys. Lett.* **2001**, *336*, 53.

(5) Liu, Z. Q.; Xie, S. S.; Sun, L. F.; Tang, D. S.; Zhou, W. Y.; Wang, C. Y.; Liu, W.; Li, Y. B.; Zou, X. P.; Wang, G. *J. Mater. Res.* **2001**, *16*, 683.

(6) Hu, W. B.; Zhu, Y. Q.; Xu, W. G. *Sci. China Ser. B* **2002**, *45*, 389.

(7) Hu, J. Q.; Jiang, Y.; Meng, X. M.; Lee, C. S.; Lee, S. T. *Chem. Phys. Lett.* **2003**, *367*, 339.

(8) Martin, C. R. *Chem. Mater.* **1996**, *8*, 1739.

(9) Satishkumar, B. C.; Govindaraj, A.; Vogl, E. M.; Basumallick, L.; Rao, C. N. R. *J. Mater. Res.* **1997**, *12*, 604.

(10) Lakshmi, B. B.; Patrissi, C. J.; Martin, C. R. *Chem. Mater.* **1997**, *9*, 2544.

(11) Zhang, M.; Bando, Y.; Wada, K. *J. Mater. Res.* **2000**, *15*, 187.

(12) Obare, S. O.; Jana, N. R.; Murphy, C. J. *Nano Lett.* **2001**, *1*, 601.

(13) Yin, Y.; Lu, Y.; Sun, Y.; Xia, Y. *Nano Lett.* **2002**, *2*, 427.

(14) Mitchell, D. T.; Lee, S. B.; Trofin, L.; Li, N.; Nevanen, T. K.; Soderlund, H.; Martin, C. R. *J. Am. Soc. Chem.* **2002**, *124*, 11864.

(15) Hu, J. Q.; Meng, X. M.; Jiang, Y.; Lee, C. S.; Lee, S. T. *Adv. Mater.* **2003**, *15*, 70.

(16) Kovtyukhova, N. I.; Mallouk, T. E.; Mayer, T. S. *Adv. Mater.* **2003**, *15*, 780.

(17) Liang, C.; Shimizu, Y.; Sasaki, T.; Umehara, H.; Koshizaki, N. *J. Mater. Chem.* **2004**, *14*, 248.
(18) Wang, L. S.; Desai, S. R.; Wu, H.; Nichloas, J. B. *Z. Phys. D* **1997**, *36*, 40.
(19) Iraqi, M.; Goldberg, N.; Schwarz, H. *J. Phys. Chem.* **1993**, *97*, 11371.
(20) Goldberg, N.; Iraqi, M.; Koch, W.; Schaltz, H. *Chem. Phys. Lett.* **1994**, *225*, 404.
(21) Lafargue, P. E.; Gaumet, J. J.; Muller, J. F. *J. Mass Spectrom.* **1996**, *31*, 623.
(22) Wang, L. S.; Wu, H.; Desai, S. R.; Fan, J.; Colson, S. D. *J. Phys. Chem.* **1996**, *100*, 8697.
(23) Zhao, L.; Zhu, L.; Zhang, J.; Li, Y.; Sheng, J.; Zhang, B.; Wang, J. *Chem. Phys. Lett.* **1996**, *255*, 142.
(24) Wang, L. S.; Nicholas, J. B.; Dupuis, M.; Wu, H.; Colson, S. D. *Phys. Rev. Lett.* **1997**, *78*, 4450.
(25) Altman, I. S.; Lee, D.; Chung, J. D.; Song, J.; Choi, M. *Phys. Rev. B* **2001**, *63*, 161402.
(26) Glinka, Y. D.; Lin, S. H.; Lin, Y. T.; Chen, Y. T. *Phys. Rev. B* **2000**, *62*, 4733.
(27) Uchino, T.; Aboshi, A.; Kohara, S.; Ohishi, Y.; Sakashita, M.; Aoki, K. *Phys. Rev. B* **2004**, *69*, 155409.
(28) Snyder, L. C.; Raghavachari, K. *J. Chem. Phys.* **1984**, *80*, 5076.
(29) Boldyrev, A. I.; Simons, J. *J. Phys. Chem.* **1993**, *97*, 5875.
(30) Sommerfeld, T.; Scheller, M. K.; Cederbaum, L. S. *J. Chem. Phys.* **1995**, *103*, 1057.
(31) Harkless, J. A. W.; Stillinger, D. K.; Stillinger, F. H. *J. Phys. Chem.* **1996**, *100*, 1098.
(32) Nayak, S. K.; Rao, B. K.; Khanna, S. N.; Jena, P. *J. Chem. Phys.* **1998**, *109*, 1245.
(33) Chelikowsky, J. R. *Phys. Rev. B* **1998**, *57*, 3333.
(34) Xu, C.; Wang, W.; Zhang, W.; Zhuang, J.; Liu, L.; Kong, Q.; Zhao, L.; Long, Y.; Fan, K.; Qian, S.; Li, Y. *J. Phys. Chem. A* **2000**, *104*, 9518.
(35) Nedelec, J. M.; Hench, L. L. *J. Non-Cryst. Solids* **2000**, *277*, 106.
(36) Chu, T. S.; Zhang, R. Q.; Cheung, H. F. *J. Phys. Chem. B* **2001**, *105*, 1705.
(37) Zhang, R. Q.; Chu, T. S.; Cheung, H. F.; Wang, N.; Lee, S. T. *Phys. Rev. B* **2001**, *64*, 113304.
(38) Flikkema, E.; Bromley, S. T. *Chem. Phys. Lett.* **2003**, *378*, 622.
(39) Flikkema, E.; Bromley, S. T. *J. Phys. Chem. B* **2004**, *108*, 9638.
(40) Wales, D. J.; Doye, J. P. K. *J. Phys. Chem. A* **1997**, *101*, 5111.
(41) Song, J.; Choi, M. *Phys. Rev. B* **2002**, *65*, 241302.
(42) Umari, P.; Gonze, X.; Pasquarello, A. *Phys. Rev. Lett.* **2003**, *90*, 027401.
(43) Lu, W. C.; Wang, C. Z.; Ho, K. M. *Chem. Phys. Lett.* **2003**, *378*, 225.
(44) Lu, W. C.; Wang, C. Z.; Nguyen, V.; Schmidt, M. W.; Gordon, M. S.; Ho, K. M. *J. Phys. Chem. A* **2003**, *107*, 6936.
(45) Zhao, M. W.; Zhang, R. Q.; Lee, S. T. *Phys. Rev. B* **2004**, *69*, 153403.
(46) Bromley, S. T.; Zwijnenburg, M. A.; Maschmeyer, Th. *Phys. Rev. Lett.* **2003**, *90*, 035502.
(47) Sun, Q.; Wang, Q.; Jena, P. *Phys. Rev. Lett.* **2004**, *92*, 039601.
(48) Bromley, S. T.; Zwijnenburg, M. A.; Flikkema, E.; Maschmeyer, Th. *Phys. Rev. Lett.* **2004**, *92*, 039602.
(49) Zhao, M. W.; Zhang, R. Q.; Lee, S. T. *Phys. Rev. B* **2004**, *70*, 205404.
(50) Zhang, D. J.; Zhang, R. Q. *Chem. Phys. Lett.* **2004**, *394*, 437.
(51) Soler, J. M.; Artacho, E.; Gale, J. D.; García, A.; Junquera, J.; Ordejón, P.; Sánchez-Portal, D. *J. Phys.: Condens. Matter* **2002**, *14*, 2745, and references therein.
(52) Frisch, M. J.; Trucks, G. W.; Schlegel, H. B.; Scuseria, G. E.; Robb, M. A.; Cheeseman, J. R.; Zakrzewski, V. G.; Montgomery, J. A., Jr.; Stratmann, R. E.; Burant, J. C.; Dapprich, S.; Millam, J. M.; Daniels, A. D.; Kudin, K. N.; Strain, M. C.; Farkas, O.; Tomasi, J.; Barone, V.; Cossi, M.; Cammi, R.; Mennucci, B.; Pomelli, C.; Adamo, C.; Clifford, S.; Ochterski, J.; Petersson, G. A.; Ayala, P. Y.; Cui, Q.; Morokuma, K.; Malick, D. K.; Rabuck, A. D.; Raghavachari, K.; Foresman, J. B.; Cioslowski, J.; Ortiz, J. V.; Baboul, A. G.; Stefanov, B. B.; Liu, G.; Liashenko, A.; Piskorz, P.; Komaromi, I.; Gomperts, R.; Martin, R. L.; Fox, D. J.; Keith, T.; Al-Laham, M. A.; Peng, C. Y.; Nanayakkara, A.; Gonzalez, C.; Challacombe, M.; Gill, P. M. W.; Johnson, B.; Chen, W.; Wong, M. W.; Andres, J. L.; Gonzalez, C.; Head-Gordon, M.; Replogle, E. S.; Pople, J. A. *Gaussian 98*, Revision A.7; Gaussian, Inc.: Pittsburgh, PA, 1998.
(53) Becke,A. D. *J. Chem. Phys.* **1993**, *98*, 5648.
(54) Lee, C.; Yang, W.; Parr. R. G. *Phys. Rev. B* **1988**, *37*, 785.
(55) Perdew, J. P.; Burke, K.; Ernzerhof, M. *Phys. Rev. Lett.* **1996**, *77*, 3865.
(56) Weiss, A. *Z. Anorg. Allg. Chem.* **1954**, *276*, 95.
(57) Chaing, C. M.; Zegarksi, B. R.; Dubois, L. H. *J. Phys. Chem.* **1993**, *97*, 6948.
(58) Ferrari, A. M.; Garrone, E.; Spoto, G.; Ugliengo, P.; Zecchina, A. *Surf. Sci.* **1995**, *323*, 151.
(59) Bakaev, V. A.; Steele, W. A. *J. Chem. Phys.* **1999**, *111*, 9803.
(60) Ceresoli, D.; Bernasconi, M.; Iarlori, S.; Parrinello, M.; Tosatti, E. *Phys. Rev. Lett.* **2000**, *84*, 3887.
(61) Roder, A.; Kob, W.; Binder, K. *J. Chem. Phys.* **2001**, *114*, 7602.
(62) Benoit, M.; Ispas, S.; Tuckerman, M. E. *Phys. Rev. B* **2001**, *64*, 224205.
(63) Levien, L.; Prewitt, C. T.; Weidner, D. J. *Am. Mineral.* **1980**, *65*, 920.
(64) Andersson, M. P.; Uvdal, P. *J. Phys. Chem. A* **2005**, *109*, 2937.
(65) Zhu, T.; Li, J.; Yip, S.; Bartlett, R. J.; Trickey, S. B.; Deleeuw, N. H. *Mol. Simul.* **2003**, *29*, 671.
(66) Kronik, L.; Fromherz, R.; Ko, E.; Ganteför, G.; Chelikowsky, J. R. *Nature Mater.* **2002**, *1*, 49.